

Polarized Reflection Spectra of Perchlorate-Doped Oriented Polyacetylene

Takayuki MIYAMAE,* Masaaki SHIMIZU, and Jiro TANAKA†

Department of Chemistry, Faculty of Science, Nagoya University, Chikusa-ku, Nagoya 464-01

† Department of Materials Science, Faculty of Science, Kanagawa University, Hiratsuka, Kanagawa 259-12

(Received May 11, 1994)

Polarized reflection spectra of a highly oriented new type polyacetylene doped with perchlorate are presented. From the reflection spectra, measured from far infrared to ultraviolet regions, the optical conductivity spectra are obtained by Kramers–Kronig analysis. Three stages of doping are recognized from a spectral analysis. (1) $0 < y < 0.02$, where the charged soliton band is dominant; (2) $0.02 < y < 0.04$, the spectra change completely and the polaron band begins to grow; (3) $0.045 < y$, the spectral characteristic of metallic phase appears. Three-dimensional interaction of the polaron chain is found to be essential for appearance of metallic conductivity. The origin of metallic properties is discussed from the change of spectra at different dopant concentration. The effect of orientation of polyacetylene chain on the spectra is discussed.

Improvement of conductivity of iodine doped polyacetylene film was achieved by Naarmann and Theophilou¹⁾ and Tsukamoto et al.²⁾ by the invention of an aged catalyst. The new type polyacetylene (N-PA) made by the new catalyst has a higher density (1.15 g cm^{-3}) and a larger elongation ratio ($l/l_0 \approx 8$) compared to polyacetylene made by the conventional Shirakawa method (S-PA).³⁾ In the N-PA the polymer chain is more ordered by stretching and the interfibril contact may be increased.

Anisotropy of conductivity is expected in the oriented film, so the optical study with a polarized light will be of great help to analyze the electronic structure of the doped polymer. Only a few studies have been presented on the orientational effect of optical anisotropy of conducting polymer.⁴⁾ In our previous study on the iodine-doped oriented N-PA, we found the change of polarized reflection spectra with the doping level. The transition to metallic state has been found above a particular dopant concentration.⁵⁾ The optical conductivity spectra showed that the free carriers with fairly long lifetime (ca. 10^{-13} s) were formed in the heavily doped N-PA.

In this paper we will present the polarized reflection spectra of the perchlorate doped highly oriented N-PA film from far-infrared to ultraviolet regions. The optical conductivity spectra are calculated by the Kramers–Kronig transformation of the reflection spectra. Perchlorate ion is a suitable acceptor for spectral studies, since it has no conspicuous absorption band in the visible or near IR region. The optical conductivity spectra are analyzed by a simple harmonic oscillator model assuming several fundamental excitations. The change of the electronic structure will be discussed based on the spectra at several doping levels. Comparison will be made with the results of iodine-doped S-PA⁶⁾ and N-PA⁵⁾ films. We will discuss the effect of stretching on the polarized spectra in connection with the electronic structure and conduction mechanism of doped polyacetylene.

Experimental

The polymerization catalyst was prepared according to the technique described by Tsukamoto et al.²⁾ The films were polymerized on a glass plate with the catalyst on it; this took place in a glove box, where argon gas was circulated through the purification system that can keep oxygen and water contents below 1.0 ppm, respectively.¹⁾ Acetylene gas of six-nine grade is passed over catalyst at -10°C at low pressure of 250 Torr (1 Torr = 133.32 Pa). The films were washed 7 times or more with toluene, then stretched inside the glove box, and finally dried in vacuo. The doping was carried out in an acetonitrile solution of copper(II) perchlorate. Twenty-five grams of copper(II) perchlorate hexahydrate ($\text{Cu}(\text{ClO}_4)_2 \cdot 6\text{H}_2\text{O}$, Nacalai tesque) was dissolved in 500 ml acetonitrile with 200 grams of molecular sieve 4A. The solution was stirred for one night and filtered, then acetonitrile was evaporated with a vacuum pump. The dried copper(II) perchlorate was dissolved in anhydrous acetonitrile ($0.005\text{--}0.1 \text{ M}$, $1 \text{ M} = 1 \text{ mol dm}^{-3}$). Polyacetylene film was immersed in the solution; the time was varied, 1 min to 2 h, for light or heavy doping. After doping, the films were washed 5 times or more with acetonitrile, and dried in vacuo. The doping levels were determined from the weight uptake. The d.c. conductivity was measured by a four probe method, applying a mechanical contact between the film and the Pt wire in the glove box. Polymerization, washing, doping, and measurements of the d.c. conductivity were carried out under argon atmosphere. The polarized reflection spectra in the far-IR region ($80\text{--}600 \text{ cm}^{-1}$) were measured with a Michelson-type interferometer constructed in this laboratory with a liq. He cooled Si-bolometer and a wire-grid polarizer. Since the sample doped with perchlorate was sensitive to air, we treated it under argon atmosphere and measured the far-IR spectra under the vacuum. The polarized reflection spectra in the IR region were measured with a KRS-5 polarizer and an FT microspectrophotometer constructed in this laboratory. The spectra in the near infrared, visible and ultraviolet regions were measured with a microspectrophotometer constructed in this laboratory.

Results and Discussion

D.C. Conductivity Figure 1 shows the dopant concentration y , $[\text{CH}(\text{ClO}_4)_y]_x$, and the d.c. conductivity

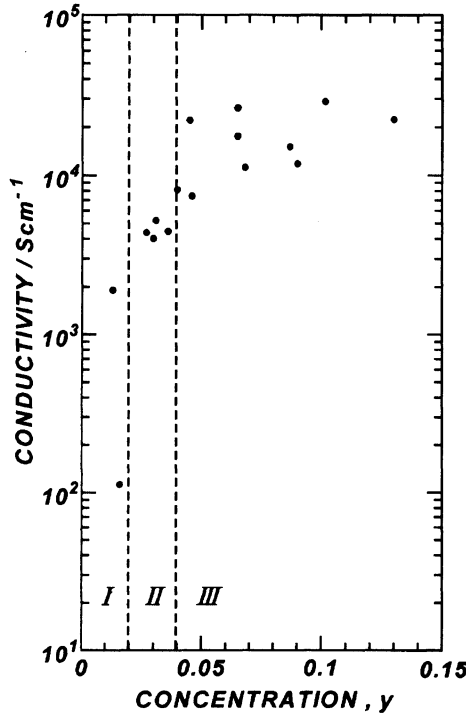


Fig. 1. Relationship between concentration of perchlorate (ClO_4^-) and conductivity of N-PA.

ity at room-temperature for the direction parallel to the stretching direction (σ_{\parallel}). The values of d.c. conductivity of perchlorate doped N-PA were two orders of magnitude larger than that of S-PA, but the relation of the conductivity to dopant concentration behaved similarly to the perchlorate doped S-PA.^{7,8)} In the region for $0 < y < 0.02$, σ_{\parallel} increased rapidly to the level of 10^3 S cm^{-1} . In the region for $0.02 < y < 0.045$, the conductivity increased gradually from 2×10^3 to 10^4 S cm^{-1} . Finally, in the region $y > 0.045$, which is the “heavily doped” regime, the conductivity saturated and the top value was dependent on the sample quality. We obtained the highest conductivity value (σ_{\parallel}) of perchlorate doped N-PA at $3 \times 10^4 \text{ S cm}^{-1}$.

Reflection Spectra. Figure 2 shows the polarized reflection spectra for the parallel and perpendicular to the stretching direction of perchlorate doped N-PA films, $[\text{CH}(\text{ClO}_4)_y]_x$, for undoped and three different dopant concentrations which correspond to the three doping stages noted in the previous section. The reflectance of the lightly ($y=0.013$) and medium ($y=0.036$) doped films were lower than those of the heavily doped film ($y=0.045$) for the whole measured region. The reflection spectrum of undoped film exhibited a peak at 17000 cm^{-1} , characteristic of the interband transition of polyacetylene. In the lightly doped film, this peak intensity decreased and a new broad band appeared in the near infrared region at 5000 cm^{-1} (band No. 6) and a sharp one at 1360 cm^{-1} (band No. 4). In the heavily doped film, the spectrum for the parallel direction exhibited a high reflectance reaching nearly

100 percent in the far-IR region (band No. 0) and a broad band at around 400 cm^{-1} (band No. 1). Along the perpendicular direction, sharp peaks are found at 1030 and 1120 cm^{-1} ; the former one is due to one of the soliton bound modes⁹⁾ and the latter one is due to the bending mode of perchlorate. In spite of difference in the d.c. conductivity, the reflection spectra of further doped films, $y=0.068$ ($\sigma_{\parallel}=11200 \text{ S cm}^{-1}$), $y=0.102$ ($\sigma_{\parallel}=28700 \text{ S cm}^{-1}$) and $y=0.132$ ($\sigma_{\parallel}=6600 \text{ S cm}^{-1}$), have intensities and positions of peaks similar to the values for the curve of $y=0.045$ over the whole measured region within measurement error. This behavior is in good agreement with the result of the d.c. conductivity shown in Fig. 1.

Optical Conductivity and Simple Harmonic Oscillator Model. The Kramers-Kronig transformation of the reflection spectra were calculated to obtain the optical conductivity spectra, $\sigma(\omega)$. The calculated result is shown in Fig. 3. The optical conductivity spectra $\sigma(\omega)$ in cgs units are given by the imaginary part of the dielectric function, $\varepsilon_2(\omega)$ as

$$\sigma(\omega) = \frac{\omega}{4\pi} \varepsilon_2(\omega). \quad (1)$$

By using a simple harmonic oscillator model, the dielectric function $\varepsilon(\omega)$ is given by

$$\varepsilon(\omega) \equiv \varepsilon_1(\omega) + i\varepsilon_2(\omega), \quad (2)$$

$$= \varepsilon_{\text{core}} + \sum_{j=0}^7 \frac{\Omega_j^2 [(\omega_j^2 - \omega^2) + i\omega\gamma_j]}{(\omega_j^2 - \omega^2)^2 + \omega^2\gamma_j^2}, \quad (3)$$

$$\Omega_j^2 = \frac{4\pi f_j N e^2}{m_e}, \quad (4)$$

where ω_j , γ_j , and f_j are the resonance frequency, the band width, and the oscillator strength of the j -th transition, respectively. N is the number of species for the transition per unit volume and m_e is the mass of an electron. Then $\sigma(\omega)$ is given by

$$\sigma(\omega) = \sum_{j=0}^7 \frac{\Omega_j^2 \omega^2 \gamma_j}{4\pi [(\omega_j^2 - \omega^2)^2 + \omega^2 \gamma_j^2]}, \quad (5)$$

$$\equiv \frac{\sigma_0^{\text{opt}} \gamma_0^2}{\omega^2 + \gamma_0^2} + \sum_{j=1}^7 \frac{\Omega_j^2 \omega^2 \gamma_j}{4\pi [(\omega_j^2 - \omega^2)^2 + \omega^2 \gamma_j^2]}, \quad (6)$$

$$\sigma_0^{\text{opt}} \equiv \frac{\Omega_0^2}{4\pi \gamma_0} = \frac{\Omega_0^2 \tau_0}{4\pi}, \quad (7)$$

$$\Omega_0^2 = \frac{4\pi N_0 e^2}{m^*}, \quad (8)$$

where the first term of Eq. 6 is the contribution of a free carrier, τ_0 is the lifetime of free carrier related to the scattering rate by $\gamma_0=1/\tau_0$, N_0 is the number of free carriers per unit volume and m^* is the effective mass which is assumed as $m^*=m_e$ in this analysis. The values of N_0 are estimated from the fitting of $\sigma(\omega)$ in the far-infrared region and are listed in Table 1. In this analysis, the values of f_j ($j=1$ to 6) were obtained using

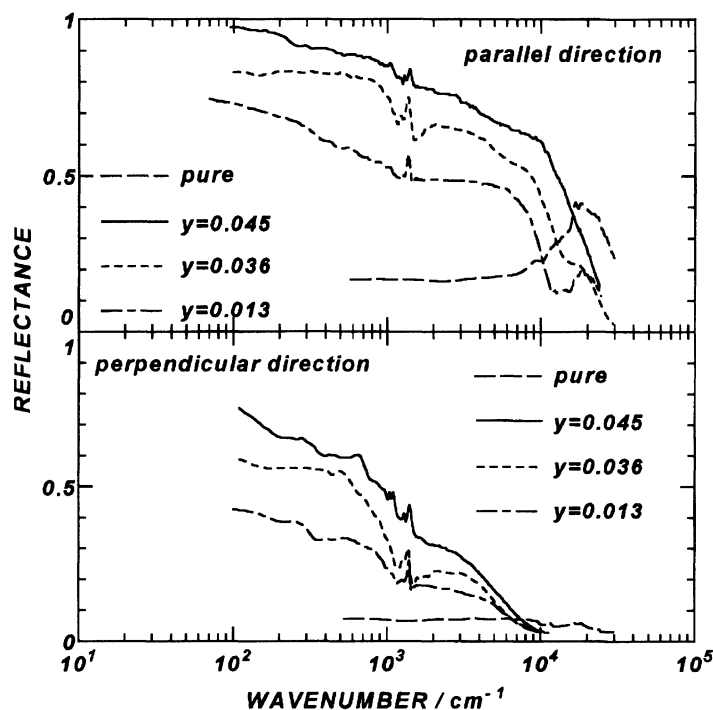


Fig. 2. Polarized reflection spectra of perchlorate-doped $\text{PA}[\text{CH}(\text{ClO}_4)_y]_x$. (a) pure N-PA; (b) $y=0.013$ ($\sigma_0^{\text{obs}}=1900 \text{ S cm}^{-1}$); (c) $y=0.036$ ($\sigma_0^{\text{obs}}=4450 \text{ S cm}^{-1}$); (d) $y=0.045$ ($\sigma_0^{\text{obs}}=22000 \text{ S cm}^{-1}$).

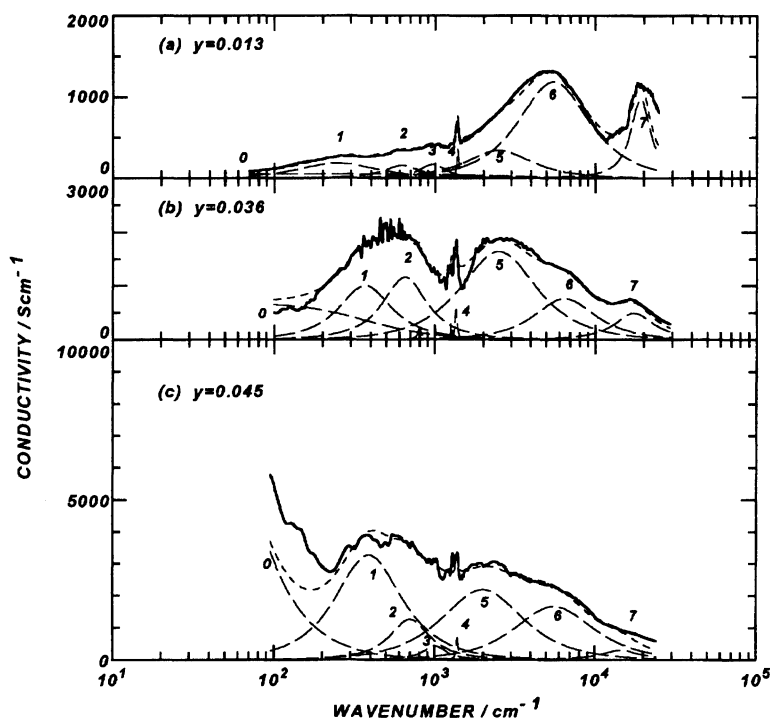


Fig. 3. Optical conductivity spectra of perchlorate-doped $\text{PA}[\text{CH}(\text{ClO}_4)_y]_x$. The polarization direction is parallel to the stretching direction. (a) $y=0.013$ ($\sigma_0^{\text{obs}}=1900 \text{ S cm}^{-1}$); (b) $y=0.036$ ($\sigma_0^{\text{obs}}=4450 \text{ S cm}^{-1}$); (c) $y=0.045$ ($\sigma_0^{\text{obs}}=22000 \text{ S cm}^{-1}$).

$N = n_{\text{cs}} \times N_{\pi}$ for the film $y > n_{\text{cs}}$, where n_{cs} is the dopant concentration above which the polaron band appears.^{5,6)} The value of n_{cs} is taken as 0.025. For $y < n_{\text{cs}}$, $N = y \times N_{\pi}$. N_{π} is the number of carbon $2p\pi$ electron in unit volume.

The choice of N implies that the values of f_1, \dots, f_6 are determined for the chain of 40 carbon atoms. Since the origin of the band No. 7 is the interband transition of polyacetylene, the values of f_7 were obtained using

Table 1. Optical Parameters Obtained with Simulation of Optical Conductivity Spectra (Parallel Direction)

					$y=0.013$		$y=0.036$		$y=0.045$			
$\sigma_0^{\text{obs}}/\text{S cm}^{-1}$					1900		4450		22000			
$\sigma_0^{\text{opt}}/\text{S cm}^{-1}$					50		700		28000			
Ω_0/cm^{-1}					3000		4000		7700			
τ/s					1.77×10^{-15}		1.39×10^{-14}		1.50×10^{-13}			
$n_{\text{cs}} \times N_{\pi}/\text{cm}^{-3}$					6.00×10^{20}		1.00×10^{21}		1.16×10^{21}			
N_0/cm^{-3}					1.01×10^{20}		1.79×10^{20}		6.63×10^{20}			
$\varepsilon_{\text{core}}$					4.0		2.5		3.6			
j	$\frac{\omega_j}{\text{cm}^{-1}}$	$\frac{\gamma_j}{\text{cm}^{-1}}$	f_j	$\frac{\langle r \rangle}{\text{\AA}}$	$\frac{\omega_j}{\text{cm}^{-1}}$	$\frac{\gamma_j}{\text{cm}^{-1}}$	f_j	$\frac{\langle r \rangle}{\text{\AA}}$	$\frac{\omega_j}{\text{cm}^{-1}}$	$\frac{\gamma_j}{\text{cm}^{-1}}$	f_j	$\frac{\langle r \rangle}{\text{\AA}}$
1	250	360	0.075	3.04	370	340	0.23	4.37	390	460	0.87	8.28
2	620	400	0.070	1.86	650	500	0.39	4.29	700	480	0.35	3.92
3	960	450	0.085	1.65								
4	1380	50	0.020	0.67	1360	50	0.02	0.67	1380	50	0.02	0.67
5	2500	3000	1.15	3.76	2500	3500	3.85	6.88	2000	3000	3.85	7.64
6	5500	7000	9.30	7.21	6500	7000	3.60	4.13	5600	8000	7.70	6.50
7	19000	6500	0.092	0.39	17500	12000	0.086	0.39	14500	10000	0.043	0.30

$N = N_{\pi}$.

Changes of Spectra with Doping. In Fig. 3 we show the optical conductivity spectra of (a) $y=0.013$, (b) $y=0.036$, and (c) $y=0.045$ films by the solid lines for the direction parallel to the stretching direction. The optical conductivity increased with the dopant concentration, particularly in the far infrared region. At a low doping level of $y=0.013$, the d.c. conductivity was 1900 S cm^{-1} , it increased to 4450 S cm^{-1} at $y=0.036$ and reached a maximum value of 22000 S cm^{-1} at $y=0.045$. The growing of the d.c. conductivity is intimately connected with the enhancement of the far infrared optical conductivity.

The dashed lines in Fig. 3 illustrate the fitted spectra by a simple harmonic oscillator model and the broken lines denote the contributions of each transition numbered from 0 to 7. The parameters for the fitting are shown in Table 1. In the near infrared region, better fitting curves than the previous analysis⁵⁾ are obtained by considering two transitions, Nos. 5 and 6. They are at about 2000 cm^{-1} (No. 5) and 6000 cm^{-1} (No. 6), respectively. Besides these strong bands, a broad band around 400 cm^{-1} (No. 1) and a small sharp peak at 1360 cm^{-1} (No. 4) were found. The band No. 4 was assigned to the characteristic C-H bending modes of the charged soliton structure. In the structural model of the charged soliton it was proposed that the odd-numbered CH chains are coordinated by a dopant.¹⁰⁾

In the lightly doped film of $y=0.013$, the bands of 6000 cm^{-1} (No. 6) and 1360 cm^{-1} (No. 4) were predominant, as shown in Fig. 3(a). In the initial stage of doping, a measurable conductivity appeared. Yang et al. showed that the doped film is diamagnetic at this concentration range;⁸⁾ their result is consistent with the result that the charged soliton structure, which is diamagnetic, is predominant at $y < 0.02$. The metallic state is not yet realized if the doping levels are $y < 0.02$.

From the intensity of the visible band, the content of the undoped region can be estimated; then the doped region is evaluated as 67 percent of the total chain at $y=0.013$. We assume the perchlorate doped polyacetylene has a similar structure to the iodine doped film of $(\text{UP})_n$ structure (Fig. 4(b)) proposed by Baughman's group.¹¹⁾ Here, the U layer is comprised of only undoped polyacetylene chain and the P layer is partially filled with perchlorate ions. Then each unit cell includes three chains, so one of the three chains remains undoped at this concentration. This argument is consistent with the previous studies on Na-doped,^{12,13)} iodine-doped S-PA⁶⁾ and perchlorate doped S-PA.⁸⁾ The number of carbon atoms per dopant is found as 51 carbon atoms in the two doped chains. This result shows that each dopant in the charged soliton chain influences over a fairly long distance.

By increasing the doping level to $y=0.036$, the conductivity increased to $\sigma_{\parallel}=4450 \text{ S cm}^{-1}$, and two new bands appeared in the 400 cm^{-1} (No. 1) and 2000 cm^{-1} (No. 5) regions (Fig. 3(b)). They are indications of a new species produced, and the species was called polson.¹⁴⁾ The structural model of polson was proposed: As follows the odd numbered CH chains are coordinated by the two dopants from the same side. The polson structure has an electronic excited state at 2000 cm^{-1} and vibrational modes at 600 cm^{-1} regions. At $y=0.036$, the undoped part of the chain still remained 33 percent, as estimated from the intensity of 16000 cm^{-1} band. If we assume $(\text{UP})_n$ structure at $y=0.036$, one third of polyacetylene chain is undoped, another chain has a polson structure: The unit is composed of 23 carbon atoms, and the third chain has a charged soliton structure.

Band No. 1 has been assigned to the pinned mode of the free carrier. Woo et al.¹⁵⁾ observed a strong broad band around 400 cm^{-1} in the iodine-doped N-PA and its

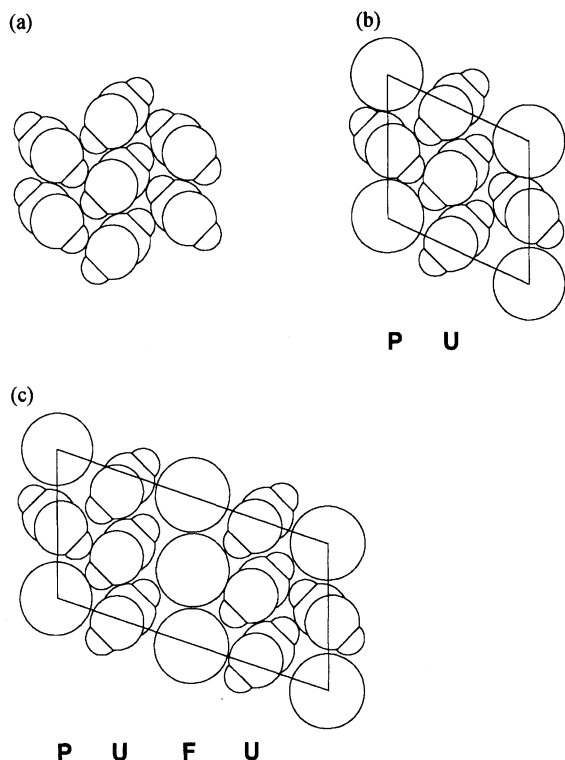


Fig. 4. Illustration of Baughman's model for doped polyacetylene projected along the chain axis for polyacetylene. (a) undoped $(CH)_x$. (b) $(UP)_n$ lattice for light doped polyacetylene. (c) $(UPUF)_n$ lattice for doped until metallic region. Large circles illustrate dopant column.

intensity increased with decreasing temperature. They attributed this to the pinning of the free carrier. From the present analysis, it appears that they showed that the intensity of the free carrier band (N_0) was transferred to band No. 1 (f_1) by lowering temperature.

By further doping to $y=0.045$, the optical conductivity rises steeply toward $\omega \rightarrow 0$; it indicates that the number of the free carriers increased significantly, which is consistent with the increased d.c. conductivity ($2.2 \times 10^4 \text{ Scm}^{-1}$). A similar feature was shown by Leising in AsF_5 -doped Durham-route polyacetylene.¹⁶⁾ Above $y > 0.045$, the undoped chain remains less than 20 percent; accordingly, the metallic property is apparent when more than 80 percent of the chains are doped to form polson chains. The number of carbon atoms per dopant is 9.5 if we assume that the polson is formed on two of five polyacetylene chains in $(UPUF)_n$ of Baughman's model (Fig. 4(c)).¹¹⁾ Here the F layer is completely filled with perchlorate ions. These results indicate that the metallic state is realized when a polson lattice is formed on two-fifths of the polyacetylene chain in $(UPUF)_n$ lattice. Moreover, the d.c. conductivity reaches a maximum value at this level and saturates above this.

In the previous report,¹⁷⁾ we showed by the ultraviolet photoemission spectra that the density of states at Fermi level were found in the heavily perchlorate

doped N-PA, at the conductivity level of more than 10^4 Scm^{-1} . The appearance of a strong free carrier band in the far infrared region and the high d.c. conductivity are consistent with the result of UPS spectra.

The rapid increase of $\sigma(\omega)$ in the far-IR region also indicates that the free carriers have a long lifetime of $\tau_0 \approx 1.5 \times 10^{-13} \text{ s}$, since the position of the spectral decay near $\omega \approx 100 \text{ cm}^{-1}$ means a small half-bandwidth, γ_0 , that is, the long lifetime (τ_0) of the free carrier. Following the Drude theory, the d.c. conductivity (σ_0) is described by the number of free carriers (N_0) and their lifetime (τ_0), as follows:

$$\sigma_0 = \frac{N_0 e^2 \tau_0}{m^*}. \quad (9)$$

The high conductivity of N-PA at $y > 0.045$ is correlated to the increased N_0 and long lifetime τ_0 . This result is in good agreement with the previous one on the iodine-doped N-PA.⁵⁾ The number of carbon $2p\pi$ electrons in a unit volume of polyacetylene is $4.6 \times 10^{22} \text{ cm}^{-3}$. Assuming $m^* = m_e$, the number of free carriers (N_0) at $y = 0.045$ was $6.63 \times 10^{20} \text{ cm}^{-3}$ (Table 1) and it increase to $1.43 \times 10^{21} \text{ cm}^{-3}$ at the top doping of $y = 0.136$. These numbers showed that one free carrier is formed for about 30 carbon atoms. Infact, the N_0 may be increased by a factor of m^*/m_e and the number of carbon atoms for the free carrier may be reduced by the same factor. Anyway, the heavily doped polyacetylene is characterized as a system with a small number of free carriers.

In Fig. 5, the intensities for each band are compared by the ratio of oscillator strengths at different dopant content, where the oscillator strengths (f_j) are calibrated by the values of lightly doped film of $y = 0.013$, where the charged soliton is the main product. From Fig. 5, the transitions are classified into three types. First, the f_4 and f_6 of the charged soliton remain constant even with the increase of dopant; this shows that the content of the charged soliton is constant for all dopant level of $y > 0.013$. The strengths of the bands No. 1 and 0 show a rapid increase above $y = 0.036$, like the rise of the d.c. conductivity. Both the free carrier band (N_0) and far-IR band (f_1) are the excitation of free carriers, since the spectral behavior is consistent with the d.c. conductivity. These bands are enhanced by stretching with the increase of the interfibril contact. The oscillator strengths, f_2 and f_5 , are enhanced at $y = 0.036$, but keeps constant above this level. Band Nos. 5 and 2 are excitations of polson unit, since it increases at $y = 0.036$ along with N_0 and f_1 . Above $y > 0.045$, many polson chains are formed and the inter-polson chain interaction is enhanced because more than two polyacetylene chains in the $(UPUF)_n$ structure are transformed to polson chains. The increase of conductivity may be correlated with the interaction between the polson chains between neighboring chains.

If we assume the chain structure at $y = 0.045$ is

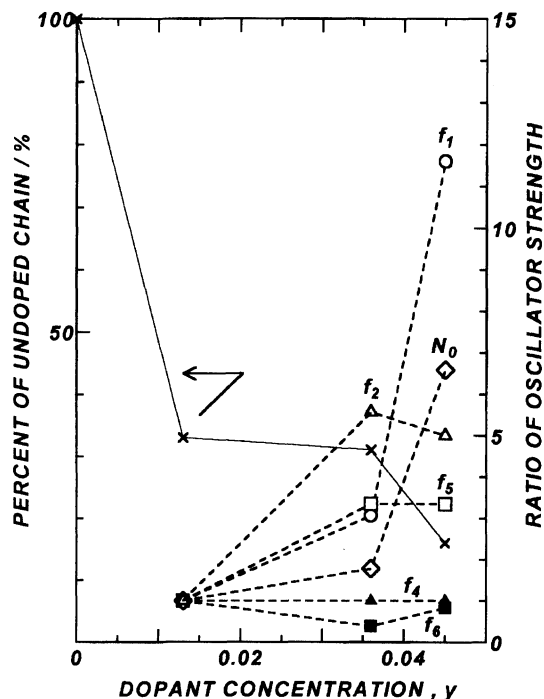


Fig. 5. Relationship between concentration of perchlorate ion (ClO_4^-) and oscillator strength of transitions which are normalized at the transition intensities of the sample of $y=0.013$.

(UPUF) $_n$, the undoped part is evaluated from the 16000 cm^{-1} band as 20 percent. Accordingly four-fifths of the (UPUF) $_n$ chains are doped. Furthermore, if we assume that half of the doped chains have a polson structure, each polson, which has two dopants, is comprised of 21 carbon atoms. The smallest polson structure contains thirteen carbon atoms; therefore, further doping can proceed to the level of $y=0.136$ by increasing the dopant content.¹⁸⁾

Anisotropy of Spectra. In Fig. 6 we show the optical conductivity spectra for the perpendicular direction at (a) $y=0.013$, (b) $y=0.036$, and (c) $y=0.045$, and the parameters obtained from the fitting are shown in Table 2.

From the optical conductivity spectra of $y=0.045$ (Fig. 3(c) and Fig. 6(c)), the dichroic ratios of each band, f_1 (390 cm^{-1}), f_2 (700 cm^{-1}), f_4 (1360 cm^{-1}) and f_5+f_6 , are 35:1, 7:1, 13:1, and 2.5:1, respectively. To compare with the previous study of iodine-doped N-PA,⁵⁾ we have to combine bands No. 5 and No. 6. It shows that the dichroic ratios of these bands have almost the same ratios compared with the bands of iodine-doped N-PA.⁵⁾ In the heavily iodine doped sample ($\text{CHI}_{0.16}$) $_x$, the corresponding ratios were 38:1, 10:1, 6.3:1, and 3:1, respectively.

The difference in dichroic ratios among these bands gives an insight into the nature of the transition. Band No. 1 is more parallel polarized to the elongated direction than band Nos. 2 and 4. The dichroic ratio of the free carrier band No. 0 is 26:1. The ratio is compara-

ble to that of band No. 1. The dichroic ratios of the band Nos. 5 and 6 are 7.5:1 and 1.8:1, respectively. Although the dichroic ratio of the band Nos. 4 and 5 show almost the same value (13:1), the charged soliton mid-gap band (No. 6) has a small dichroic ratio. This result indicates that the transition dipole moment of the charged soliton mid-gap band may be inclined to the chain axis.

Effect of Stretching on the Reflection Spectra. Figure 7 shows the change of polarized reflection spectra with the draw ratio. After drawing to the ratio (l/l_0) of 4 ($y=0.045$, $\sigma_0=22000\text{ S cm}^{-1}$) and 8 ($y=0.136$, $\sigma_0=22300\text{ S cm}^{-1}$), both films were heavily doped to saturation level. The curves (a) and (d) are parallel and perpendicularly polarized reflection spectra of the draw ratio 8, while curves (b) and (e) are those of the draw ratio 4. The spectrum of unstretched heavily doped film is curve (c).

The effect of drawing on electrical conductivity of polyacetylene has been studied by many groups, and it has been established that the conductivity is increased by drawing.^{4,20)} The optical conductivity spectra (Fig. 8) clearly show that the conductivity increases toward $\omega \rightarrow 0$ in both stretched films, and the conductivity is largest for the most stretched film. The number of free carriers of stretched (draw ratio $l/l_0 \approx 4$) and unstretched N-PA ($y=0.062$, $\sigma_0=2000\text{ S cm}^{-1}$) estimated from the plasma frequencies are 6.6×10^{20} and 1.6×10^{21} , respectively, while the value for unstretched perchlorate doped S-PA⁸⁾ ($y=0.061$, $\sigma_0=700\text{ S cm}^{-1}$) was 6.1×10^{20} estimated from $N_f = (n - n_{cs})N_\pi$, where n is the dopant content. The lifetimes of the free carriers were also $1.50 \times 10^{-13}\text{ s}$ for stretched N-PA, $2.7 \times 10^{-15}\text{ s}$ for unstretched N-PA and $4.0 \times 10^{-15}\text{ s}$ for unstretched S-PA. These results clearly show that the orientation of the fibril is very important for keeping the lifetimes of free carrier longer in stretched N-PA than in unstretched ones. Elongation of the N-PA films aligned the PA chains parallel and increased interfibril contact. The lifetime of free carrier is increased by the interfibril hopping, which results in a higher conductivity than that of the unstretched N-PA. We observed the same effect: that the stretched iodine-doped N-PA showed higher conductivity than the unstretched sample at the same dopant level ($y=0.13$).²¹⁾ These results indicate that the three-dimensional interaction in the oriented film is important for the appearance of a high conductivity.

To study the orientational effect on the electronic structure of N-PA further, we introduce the orientational order parameter \overline{P}_2 which was described by Jen et al.²²⁾ We consider two coordinate systems: (1) the laboratory frame (x, y, z) fixed with respect to the N-PA film and chosen to reflect the macroscopic symmetry of the system; and (2) the molecular frame ($1, 2, 3$) fixed on the polyacetylene chain and chosen by considering the molecular symmetry. The z -axis is parallel to

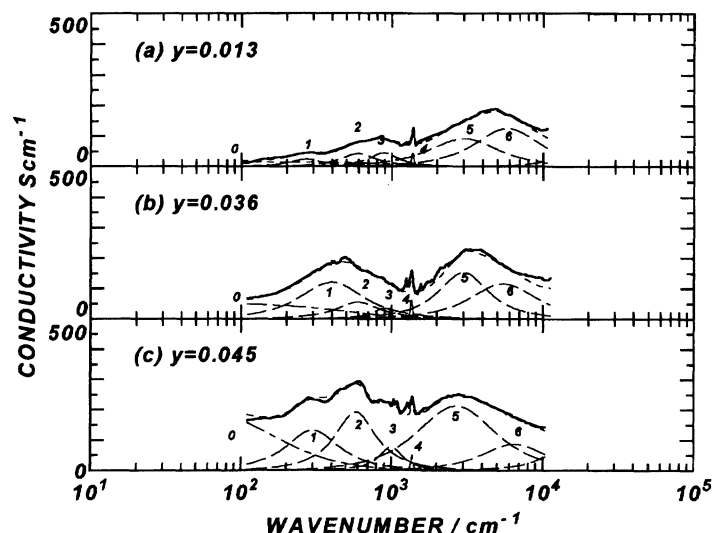


Fig. 6. Optical conductivity spectra of perchlorate-doped $\text{PA}[\text{CH}(\text{ClO}_4)_y]_x$. The polarization direction is perpendicular to the stretching direction. (a) $y=0.013$; (b) $y=0.036$; (c) $y=0.045$.

Table 2. Optical Parameters Obtained with Simulation of Optical Conductivity Spectra (Perpendicular Direction)

					$y=0.013$	$y=0.036$	$y=0.045$					
$\sigma_0^{\text{opt}}/\text{cm}^{-1}$					15	51	150					
Ω_0/cm^{-1}					1000	1200	1500					
τ/s					4.77×10^{-15}	1.13×10^{-14}	2.12×10^{-14}					
$n_{\text{cs}} \times N_{\pi}/\text{cm}^{-3}$					6.00×10^{20}	1.00×10^{21}	1.16×10^{21}					
N_0/cm^{-3}					1.12×10^{19}	1.61×10^{19}	2.52×10^{19}					
ϵ_{core}					2.4	2.4	2.3					
j	ω_j cm^{-1}	γ_j cm^{-1}	f_j	$\langle r \rangle$ \AA	ω_j cm^{-1}	γ_j cm^{-1}	f_j	$\langle r \rangle$ \AA	ω_j cm^{-1}	γ_j cm^{-1}	f_j	$\langle r \rangle$ \AA
1	270	180	0.0048	0.74	400	490	0.0397	1.75	300	300	0.025	1.60
2	600	400	0.019	0.99	600	500	0.0183	0.97	600	450	0.051	1.62
3	880	500	0.025	0.93	900	400	0.0093	0.56	1000	450	0.022	0.82
4	1380	50	0.003	0.26	1360	50	0.0024	0.23	1380	50	0.0015	0.18
5	3000	4000	0.413	2.06	3000	2800	0.290	1.72	2700	4100	0.51	2.41
6	5800	7300	1.03	2.34	5500	7000	0.548	1.75	6500	8000	4.20	1.41
7	17000	12000	0.01	0.13	14500	12000	0.01	0.15	14000	12000	0.01	0.15

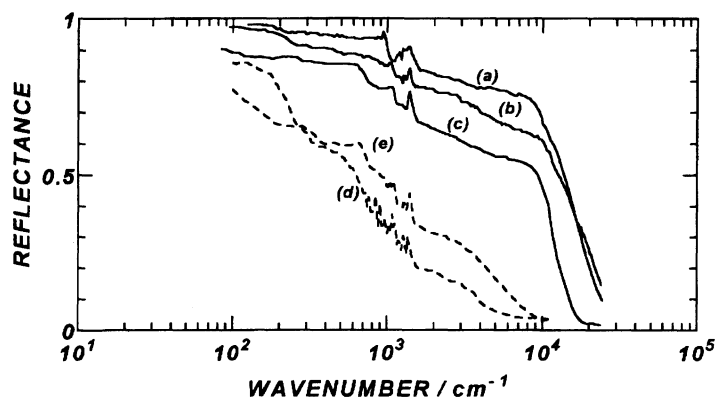


Fig. 7. Change with the stretching ratio of polarized reflection spectra at heavily doped regimes ($0.04 < y$) $[\text{CH}-(\text{ClO}_4)_y]_x$. (a) parallel direction of the sample elongated at $l/l_0 \approx 8$; (b) parallel direction of the sample of elongated at $l/l_0 \approx 4$; (c) unstretched sample; (d) perpendicular direction of the sample (a); (e) perpendicular direction of the sample (b).

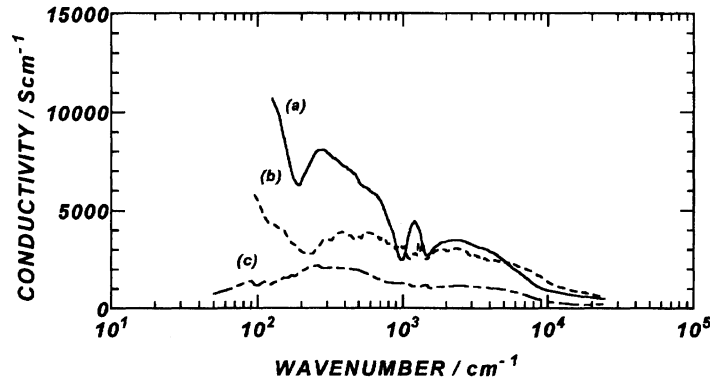


Fig. 8. Change with the draw ratio of optical conductivity spectra of perchlorate-doped N-PA. (a) parallel direction of the sample elongated at $l/l_0 \approx 8$; (b) parallel direction of the sample elongated at $l/l_0 \approx 4$; (c) unstretched sample ($y=0.062$, $\sigma_0^{\text{obs}}=2000 \text{ S cm}^{-1}$).

the stretching direction and the β -axis is parallel to the major chain axis. The orientation of a particular polyacetylene chain is described by the three Euler angles (α, β, γ) that link the two coordinate systems. The orientational order of the polymer chain is described by a distribution function $f(\alpha, \beta, \gamma)$, which can be expanded by the generalized spherical harmonics,

$$f(\alpha, \beta, \gamma) = \sum_{n=0}^{\infty} \sum_{m'=m}^n \frac{2n+1}{8\pi^2} a_{m'm}^{(n)} D_{m'm}^{(n)}(\alpha, \beta, \gamma), \quad (10a)$$

with

$$\begin{aligned} a_{m'm}^{(n)} &= \int_0^{2\pi} d\alpha \int_0^\pi \sin \beta d\beta \int_0^{2\pi} d\gamma D_{m'm}^{(n)*}(\alpha, \beta, \gamma) f(\alpha, \beta, \gamma) \\ &= \langle D_{m'm}^{(n)*}(\alpha, \beta, \gamma) \rangle, \end{aligned} \quad (10b)$$

where $D_{m'm}^{(n)}(\alpha, \beta, \gamma)$ are the Wigner matrices²³⁾ and $\langle \dots \rangle$ represents a thermal average. The distribution function, Eq. 10a, can be simplified and the number of nontrivial order parameters can be reduced by imposing the known symmetries of the individual constituent molecules and macroscopic symmetry. For a uniaxial macroscopic phase with the unique axis parallel to the z axis, the distribution function is independent of α , and only the terms with $m'=0$ contribute to the summation. If the N-PA chains are made up by cylindrically symmetrical rigid rods, we obtain

$$\begin{aligned} f_{\hat{u}}(\beta) &= \int_0^{2\pi} d\alpha \int_0^{2\pi} d\gamma f(\alpha, \beta, \gamma) \\ &= \sum_{n=\text{even}} \frac{2n+1}{2} \overline{P}_n P_n(\cos \beta), \end{aligned} \quad (11)$$

and

$$\overline{P}_n = \int_0^\pi \sin \beta d\beta P_n(\cos \beta) f_{\hat{u}}(\beta) = \langle P_n(\cos \beta) \rangle, \quad (12)$$

where $P_n(\cos \beta)$ are the Legendre polynomials and \hat{u} is the unit vector along the symmetry axis of the molecule. The order parameter \overline{P}_2 vanishes in isotropic media, takes non-zero values in the ordered media, and saturates to unity when the chain is completely aligned. The dichroic ratio R is given by using \overline{P}_2 ,

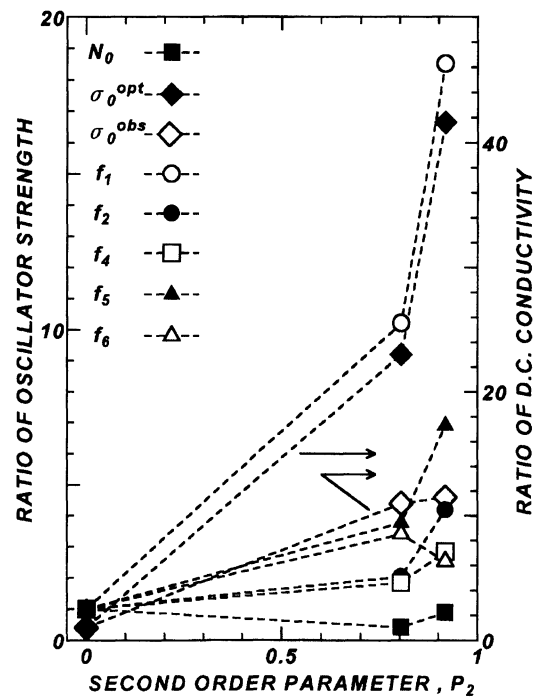


Fig. 9. Comparisons of the ratio of oscillator strength and the d.c. conductivity, which are normalized at the intensities of unstretch sample, of each intensity about the order parameter \overline{P}_2 .

$$R = \frac{1 + 2\overline{P}_2}{1 - \overline{P}_2}. \quad (13)$$

The order parameter \overline{P}_2 of the polymer chain in the films of draw ratio 4 and 8 are estimated by the dichroic ratio of the charged soliton characteristic band at 1360 cm^{-1} , because it appears for whole doping range and its polarization is believed to be parallel to the chain axis.²⁴⁾ The order parameters are obtained according to the following equations;

$$\overline{P}_2 = \frac{R - 1}{R + 2}. \quad (14)$$

The order parameters are calculated from curves of Fig. 7(a)(Fig. 8(a)) and Fig. 7(b)(Fig. 8(b)) to be 0.91

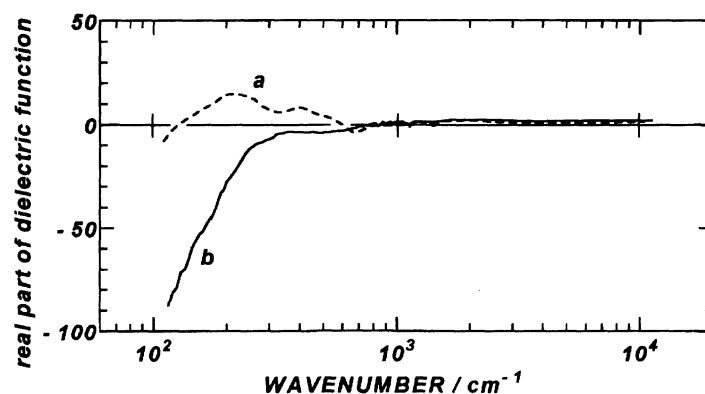


Fig. 10. Change of the real part (ϵ_1) of dielectric function with stretching (perpendicular direction); (a) $\overline{P}_2=0.82$, (b) $\overline{P}_2=0.91$.

and 0.82, respectively.

Figure 9 shows the change of oscillator strength of each transition and the change of the conductivity with the order parameter, where the values are normalized to unity for the values of unstretched sample. If we assume these infrared bands have originated from the atomic vibrations and excited electronic states of the molecular unit, then by increasing the orientation of the fibril, the oscillator strength is expected to increase to three times of the value of randomly oriented fibril (oriented gas model). The transition intensity of the 600 cm^{-1} (No. 2), 1360 cm^{-1} (No. 4), and 5000 cm^{-1} (No. 6) bands at $\overline{P}_2=0.82$ and 0.91 are almost 3–5 times larger than that of unstretched sample. In contrast, the oriented gas model is no longer valid for far-IR band (No. 1) and near-IR band (No. 5), since the oscillator strength of bands Nos. 1 and 5 for the parallel direction are more than three. Band No. 5 is assigned to the polaron structure; accordingly, the polaron is found more stable in the oriented film. Each polaron structure provides an unpaired electron, which gives the origin of a metallic state. This is another reason why the oriented film is more conductive. Moreover, the far-IR No. 1 band has same behavior to the optical d.c. conductivity (σ_0^{opt}). The origin of the far-IR No. 1 band has a close relation to the free carriers. These results showed that the free carrier band and the far-IR No. 1 band both appeared as a result of many polaron chains being formed and they are aligned parallel with interchain contact. The interchain interaction is essential for appearance of metallic bands. Figure 9 also shows the change of the d.c. conductivity with the order parameter. In fact, the d.c. conductivity does not behave similarly to the optical d.c. conductivity (σ_0^{opt}). This may be caused by the fact that the d.c. conductivity includes the effect of the macroscopic defects (imperfect interfibril contact, inhomogeneity of the sample density etc.). Since we used a far-IR microscope for measurement of the reflectance, we obtained the reflection spectra of small fine regions (ca. $70\text{ }\mu\text{m}$). Therefore, the optical d.c. conductivity may reflect the intrinsic metallic conductivity.

The intrinsic metallic state for the stretched film is

found not only for the direction parallel to the chain direction but also for the direction to it perpendicular. In Fig. 10 we show the real part of the dielectric function for the perpendicular direction at different degrees of orientational order. The curve for $\overline{P}_2=0.91$ shows negative ϵ_1 value in the far-IR region; this is evidence for the free carrier existing even for the perpendicular direction. These results clearly showed that the highly oriented N-PA has a metallic interaction even for the interfibril direction. From this, the heavily doped and highly oriented N-PA is not a simple one-dimensional conductor, but is a three-dimensional conductor; the interfibril interaction perpendicular to the chain is essential for appearance of metallic conductivity. A three-dimensional variable range hopping is the most plausible mechanism for highly oriented doped polyacetylene.¹⁸⁾

When we summarize the spectral analysis, several stages are found for perchlorate doping. First, the charged soliton is formed for $y<0.02$, second the polaron unit begins to grow for $y\approx 0.03$, and finally the inter-polaron interaction occurs through the interchain contact at $y>0.04$. More than one-dimensional interaction of the polaron chain is important for the appearance of a highly conducting state of N-PA.

This research was supported by a grant in aid for International Joint Research Project from the NEDO. T. M. expresses thanks for the Fellowship of the Japan Society for the Promotion of Science for Japanese Junior Scientists. We also thank Mr. Toshiaki Noda for his thoughtful designing and ingenious glass work of our synthetic apparatus and Dr. Shinji Hasegawa of the Institute for Molecular Science for helpful comments and discussions.

References

- 1) H. Naarmann and N. Theophilou, *Synth. Met.*, **25**, 1 (1987).
- 2) J. Tsukamoto, A. Takahashi, and K. Kawasaki, *Jpn. J. Appl. Phys.*, **29**, 125 (1990).
- 3) T. Ito, H. Shirakawa, and S. Ikeda, *J. Polym. Sci.*,

Polym. Chem. Ed., **12**, 11 (1974).

4) Y. Cao, P. Smith, and A. J. Heeger, *Synth. Met.*, **41—43**, 181 (1991).

5) S. Hasegawa, M. Oku, M. Shimizu, and J. Tanaka, *Synth. Met.*, **38**, 37 (1990).

6) K. Kamiya and J. Tanaka, *Synth. Met.*, **25**, 59 (1988).
The choice of $n_{cs}=0.025$ means that the oscillator strength was evaluated for forty carbon atoms.

7) X. Q. Yang, D. B. Tanner, A. Feldblum, H. W. Gibson, M. J. Rice, and A. J. Epstein, *Mol. Cryst. Liq. Cryst.*, **117**, 267 (1985).

8) X. Q. Yang, D. B. Tanner, M. J. Rice, H. W. Gibson, A. Feldblum, and A. J. Epstein, *Solid State Commun.*, **61**, 335 (1987).

9) A. Terai, Y. Ono, and Y. Wada, *J. Phys. Soc. Jpn.*, **55**, 2889 (1986).

10) C. Tanaka and J. Tanaka, *Bull. Chem. Soc. Jpn.*, **66**, 357 (1993).

11) N. S. Murthy, G. G. Miller, and R. H. Baughman, *J. Chem. Phys.*, **89**, 2523 (1988).

12) J. Tanaka, Y. Saito, M. Shimizu, C. Tanaka, and M. Tanaka, *Bull. Chem. Soc. Jpn.*, **60**, 1595 (1987).

13) T. C. Chung, F. Moraes, J. D. Flood, and A. J.

Heeger, *Phys. Rev. B*, **29**, 2341 (1984).

14) C. Tanaka and J. Tanaka, *Synth. Met.*, **41—43**, 3709 (1991).

15) H. S. Woo, D. B. Tanner, N. Theophilou, and A. G. MacDiarmid, *Synth. Met.*, **41—43**, 159 (1991).

16) G. Leising, *Synth. Met.*, **28**, D215 (1989).

17) K. Kamiya, H. Inokuchi, M. Oku, S. Hasegawa, C. Tanaka, J. Tanaka, and K. Seki, *Synth. Met.*, **41**, 155 (1991).

18) J. Tanaka, C. Tanaka, T. Miyamae, M. Shimizu, S. Hasegawa, K. Kamiya, and K. Seki, *Synth. Met.*, in press.

19) C. Tanaka and J. Tanaka, *Synth. Met.*, **55—57**, 4377 (1993).

20) Y. Chen, K. Akagi, and H. Shirakawa, *Synth. Met.*, **14**, 173 (1986).

21) J. Tanaka, S. Hasegawa, T. Miyamae, and M. Shimizu, *Synth. Met.*, **41—43**, 1199 (1991).

22) S. Jen, N. A. Clark, P. S. Pershan, and E. B. Priestley, *J. Chem. Phys.*, **66**, 4635 (1977).

23) M. E. Rose, "Elementary Theory of Angular Momentum," Wiley, New York (1957).

24) G. Zannoni and G. Zerbi, *J. Mol. Struct.*, **100**, 505 (1983).
